

## MIT Open Access Articles

### *Investigation of abrasive saw kickback*

The MIT Faculty has made this article openly available. **Please share** how this access benefits you. Your story matters.

**Citation:** Burcat, Steven et al. "Investigation of abrasive saw kickback." International Journal of Occupational Safety and Ergonomics (July 2020): dx.doi.org/10.1080/10803548.2020.1770529 © 2020 Central Institute for Labour Protection–National Research Institute (CIOP-PIB)

**As Published:** <http://dx.doi.org/10.1080/10803548.2020.1770529>

**Publisher:** Informa UK Limited

**Persistent URL:** <https://hdl.handle.net/1721.1/128200>

**Version:** Author's final manuscript: final author's manuscript post peer review, without publisher's formatting or copy editing

**Terms of use:** Creative Commons Attribution-Noncommercial-Share Alike



# Investigation of Abrasive Saw Kickback

Steven Burcat<sup>a</sup>, Brian Yue<sup>a</sup>, Alexander Slocum<sup>a</sup> & Tal Cohen<sup>a,b,\*</sup>

<sup>a</sup>Department of Mechanical Engineering, Massachusetts Institute of Technology, USA;

<sup>b</sup>Department of Civil and Environmental Engineering, Massachusetts Institute of Technology, USA

---

## Abstract

1 Saw kickback can cause fatal injuries, but only woodcutting saws have  
2 regulations and assessment methodologies for kickback. These regulations  
3 do not apply to abrasive cutting saws, as their cutting mechanism and  
4 dominant kickback mode differ from those of woodcutting saws. This work  
5 combines theoretical and experimental tools to investigate abrasive saw  
6 kickback. A theoretical model based on frictional engagement during a  
7 pinch-based kickback event is shown to predict resultant kickback energy in  
8 good agreement with experimental measurements. These measurements  
9 were obtained using a specialized machine that generates pinch-based  
10 kickback events and measures resultant kickback energy. Upon validating  
11 the model, two representative saws, a circular cutoff saw and a chainsaw,  
12 were tested using the prototype machine to evaluate their comparative  
13 kickback risk. This work demonstrates that pinch-based kickback is a  
14 potential safety risk for abrasive cutting saw operators and provides a testing  
15 machine design and analytical framework for evaluating this risk.  
16

*Keywords:* Kickback, Safety, Saws

---

\*Corresponding author. Email: [talco@mit.edu](mailto:talco@mit.edu)

17

## 1. Introduction

18

19

20

21

22

23

24

25

26

27

28

29

30

31

32

33

Operating power tools carries inherent risk, but some hazards are more dangerous than others. Of the hazards associated with operating woodcutting chainsaws, kickback is the most common and dangerous [1-3]. Although the documentation of this hazard refers to incidents involving woodcutting chainsaws in forestry applications, kickback also causes fatal injuries on construction sites, where the use of abrasive saws for metal and concrete/masonry cutting is more prominent. While woodcutting and abrasive saws have different cutting mechanisms, as illustrated in Figure 1, operators of both types of saws can experience kickback. Kickback is defined for the purpose of this study as “a sudden, unexpected reaction occurring on the upper portion of the guidebar nose causing the guidebar to be driven up and back toward the operator,” as noted by the Chain Saw Manufacturers’ Association [4]. This “upper portion” can be defined as the kickback zone, and it is illustrated in Figure 2. While this definition refers specifically to kickback for chainsaws, it will also be used here to refer to a similar reaction for a circular cutoff saw.

34



(a) Woodcutting Chain



(b) Abrasive Chain



(c) Woodcutting Blade



(d) Abrasive Blade

35

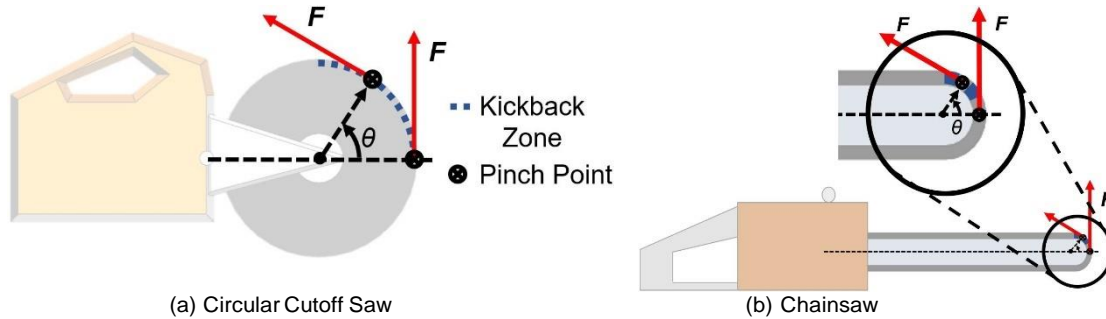
36

37

38

39

Figure 1: Visualization of woodcutting (a,c) and abrasive (b,d) cutting elements, as seen on chains (a,b) and blades (c,d). The woodcutting elements have teeth that cut into the work material, while the abrasive elements are embedded with a hard material (such as diamond) to shear through the work material.



40

(a) Circular Cutoff Saw

(b) Chainsaw

41

Figure 2: Illustration of the kickback zone on a circular cutoff saw (a) and a chainsaw (b).

42

The kickback zone is notably larger on the circular cutoff saw due to the larger blade

43

diameter. Note:  $\theta$  = angle between  $r_{co}$  and the x axis;  $F$  = force vector;  $r_{co}$  = vector from

44

the center of mass of the saw to the center of rotation of the cutting element. Labels in

45

(a) also apply to (b).

46

This kickback phenomenon is well studied for woodcutting saws due to

47

a US Consumer Product Safety Commission push to regulate woodcutting

48

chainsaws to reduce the hazard of kickback [5]. The subsequent work includes

49

the construction of kickback test machines for measuring the kickback energy

50

of these woodcutting chainsaws [1,6], simulated operator responses to the

51

occurrence of kickback [2], and brake systems for protecting operators from

52

the danger of kickback [3]. Although an increase in the number of chainsaw

53

related injuries initiated extensive investigation into reducing woodcutting

54

saw kickback [3,5], the resulting measurement techniques and safeguarding

55

methods do not apply to abrasive saws. However, a similar mandate has

56

not been made for further understanding abrasive saw kickback and how it

57

differs from woodcutting saw kickback.

58

For abrasive saws, dangerous kickback most frequently occurs on

59

construction sites during pipe cutting operations, particularly when the pipe

60

is in an excavated trench. However, when abrasive saws were tested in a

61

machine analogous to a woodcutting saw kickback machine described by

62

ANSI Standard B175.1 [6], similar levels of kickback were not observed by

63

Wu [7], despite reports of kickback in the field. A recent study by Yue [8]

64 theorized that this result is due to abrasive saws primarily experiencing a  
65 different mode of kickback whereby the cutting element is pinched in the  
66 kerf of the cut, rather than being frontally engaged by the work piece. To  
67 investigate abrasive saw kickback, a kinetics model was developed which  
68 treats the abrasive cutting engagement as a sudden frictional engagement.  
69 This model predicts the resultant motion of the saw, given assumed  
70 engagement parameters, allowing for a prediction of the resultant energy  
71 transferred to the saw's motion during a kickback event.

72 A variety of saws are used on construction sites, but they can generally  
73 be divided into two main categories: chainsaws and circular cutoff saws.  
74 Circular cutoff saws have a large diameter blade which spins on a shaft in  
75 stationary bearings. Chainsaws have a chain which moves around a  
76 stationary saw bar which has a small diameter semicircle at the nose. For  
77 this study, two representative gas-powered saws – one circular cutoff saw  
78 (Stihl TS420; Stihl USA, USA) and one chainsaw (ICS 695XL; Blount  
79 International, UA) – were used. Additionally, an electric circular cutoff saw  
80 was used for initial tuning of the physics model and validation of the  
81 machine's data collection. This approach is similar to the approach taken  
82 by Arnold and Parmigiani [9] of using electric and gas-powered saws and  
83 subsequently comparing data.

84 After Wu [7] observed and Yue [8] confirmed that the dominant kickback  
85 mode for abrasive saws is different from that of woodcutting saws, it was  
86 necessary to design a new test machine which could controllably and  
87 repeatedly produce pinch-based kickback. This machine would need to  
88 measure both the rotational and linear kinetic energy of the saw after the  
89 kickback to provide data which could be integrated into existing standards  
90 relating saw energy levels to kickback safety [6]. This work thus  
91 investigates a potential cause of kickback for abrasive power saws on work

92 sites and presents an analytical model and design of a reliable machine for  
93 measuring the kickback risk of these saws which validates the theory.

94 This manuscript is organized as follows: First, the development of the  
95 kickback model and key equations are presented. Next, the design of the  
96 test machine is discussed alongside the basic test procedure.  
97 Subsequently, test results demonstrating the validity of the of the model  
98 and utility test machine are provided. Finally, the test results using the  
99 representative gas-powered circular cutoff saw and chainsaw are provided  
100 and compared.

## 101 **2. Methodology**

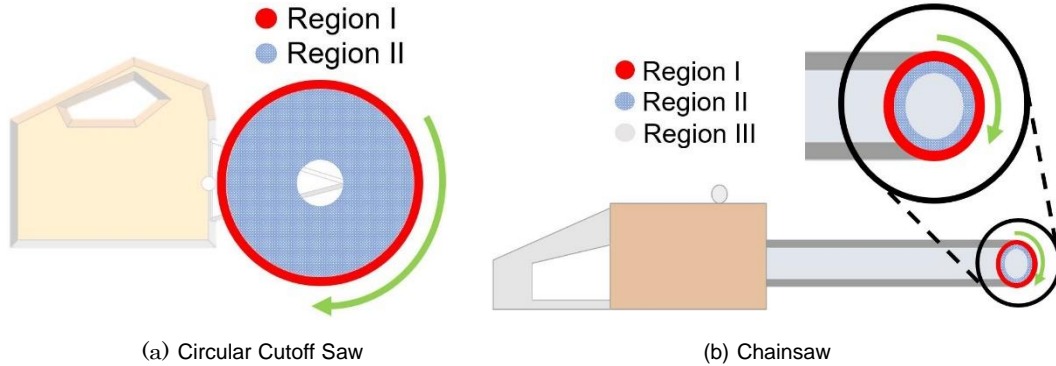
### 102 *2.1. Model*

103 The kickback phenomenon is modeled by applying a frictional contact  
104 force on the saw at a pinch point which is fixed in space. The saw is allowed  
105 to rotate and translate in the plane of the blade such that as the system  
106 evolves, the saw blade moves through the pinch point. We restrict the  
107 analysis to consider only in-plane motion following observations that confirm  
108 the out of plane motion is negligible. Boundary conditions determine  
109 geometrically when the saw has separated from the pincher, at which point  
110 rigid body motion is used to calculate the maximum linear and rotational  
111 kinetic energies of the saw.

#### 112 *2.1.1. Definitions*

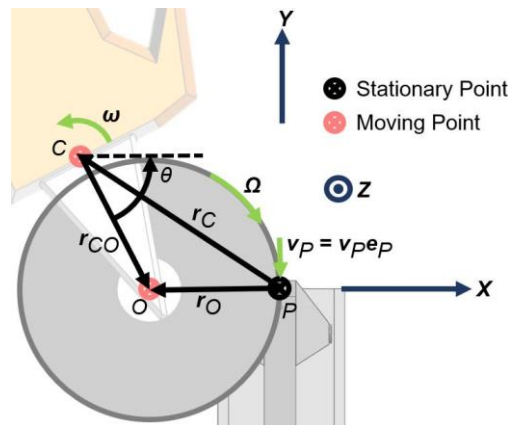
113 The saw consists of a combination of two rigid bodies: the saw body  
114 and the spinning cutting device (blade or chain). For the chainsaw, only the  
115 chain moves independently while the enclosed saw bar moves rigidly with  
116 the rest of the saw. In the model, the chainsaw cutting blade is treated as  
117 a circular ring spinning around the nose sprocket, and the rest of the saw  
118 bar region, including the area inside the ring, is treated as part of the saw

119 body. The cutting blade has two regions: the abrasive and non-abrasive  
 120 parts of the blade. Each of these regions is assigned its own effective  
 121 coefficient of friction. These regions are illustrated in Figure 3.



122 (a) Circular Cutoff Saw (b) Chainsaw

123 Figure 3: The different regions of a saw cutting blade which can be engaged during  
 124 kickback. The regions for a circular cutoff saw appear in (a), and the regions for a chainsaw  
 125 appear in (b). The chainsaw has an additional third region which moves with the saw body.



126 Figure 4: Labeled diagram showing the vectors used in the model. Note:  $\theta$  = angle  
 127 between  $r_{CO}$  and the  $x$  axis;  $\Omega$  = angular velocity of the cutting element;  $\omega$  = angular  
 128 velocity of the saw;  $C$  = the center of mass of the saw;  $O$  = the center of rotation of the  
 129 cutting element;  $r_C$  = vector from  $P$  to  $C$ ;  $r_{CO}$  = vector from  $C$  to  $O$ ;  $r_O$  = vector from  $P$  to  
 130  $O$ ;  $P$  = is the pinch engagement point;  $v_P = v_{PeP}$   
 131  $P$ .

132 A diagram illustrating the key vector definitions in the derivation of the  
 133 kickback model appears in Figure 4. The abrasive engagement force is  
 134 treated as linear friction acting on both sides of the cutting element at point

135 *P*. Thus, the force is evaluated as the product of an effective coefficient of  
 136 friction and the normal force of the pinch as

$$137 \quad \mathbf{F} = -2\mu N \mathbf{e}_P \quad (1)$$

138 where  $\mathbf{F}$  is the force vector,  $\mu$  is the effective coefficient of friction between  
 139 the spinning blade and the work material,  $N$  is the normal force of the pinch  
 140 engaging the cutting element, and  $\mathbf{e}_P$  is the unit vector pointing in the  
 141 direction of the motion of the spinning blade relative to the fixed work  
 142 material at the pinch point. Since the force is modeled as friction, it is in the  
 143  $-\mathbf{e}_P$  direction. The direction of this unit vector at any given instant is in the  
 144 direction of the velocity:

$$145 \quad \mathbf{v}_P = \mathbf{v}_C - \boldsymbol{\omega} \times \mathbf{r}_C - \boldsymbol{\Omega} \times \mathbf{r}_O \quad (2)$$

$$146 \quad \boldsymbol{\omega} = \dot{\theta} \mathbf{e}_z \quad (3)$$

$$147 \quad \boldsymbol{\Omega} = -\Omega \mathbf{e}_z \quad (4)$$

148 where the angles  $\theta$ ,  $\Omega$ , and the vectors  $\mathbf{r}_C$ ,  $\mathbf{r}_O$ , are defined in Figure 4, the  
 149 superimposed dot denotes differentiation with respect to time, and  $\mathbf{e}_z$   
 150 refers to unit vector along the z axis.

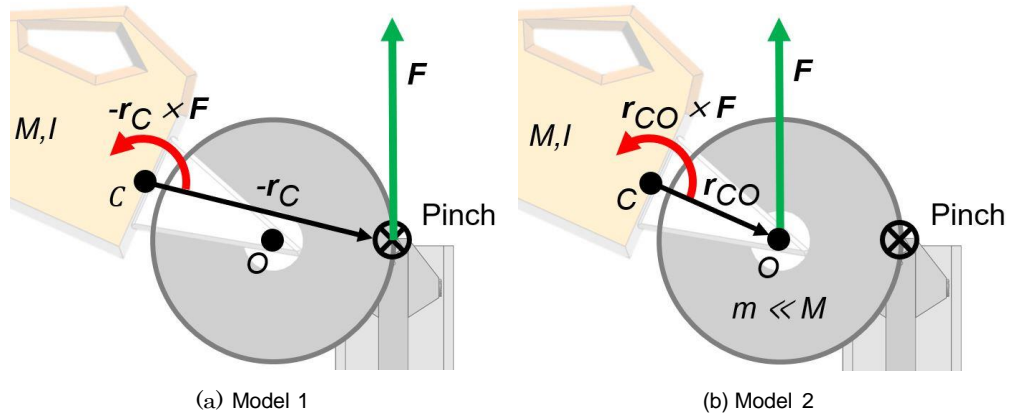
### 151 2.1.2. Simplifications

152 Each saw can be represented as two coupled bodies, the main saw  
 153 body and the moving cutting element. Because the exact coupling torque  
 154 is not known for each saw and is complex and difficult to measure, some  
 155 simplifications are made to model the system. First, since the coupling  
 156 torque between the bodies is not known, the change in the speed of the  
 157 cutting blade throughout the kickback cannot be calculated. However, the  
 158  $-\boldsymbol{\Omega} \times \mathbf{r}_O$  term in Equation (2) dominates  $\mathbf{v}_P$  for the majority of a kickback  
 159 event, even when  $\Omega$  slows down considerably. Thus, the direction of the  
 160 force,  $-\mathbf{e}_P$ , does not change significantly when the cutting blade speed  
 161 changes. To simplify the calculation of  $\mathbf{v}_P$ , a constant value is used for  $\Omega$ .



162 Note that, since  $\Omega$  is assumed constant, complete stopping of the blade,  
 163 which may be observed in extreme pinching scenarios, cannot be captured  
 164 by this model.

165 Secondly, it is desirable to simplify the system into a single rigid body  
 166 for analysis to remove the need to calculate the coupling torque. Two  
 167 separate approaches are used to create two models for the system, defined  
 168 as *Model 1* and *Model 2*, which are illustrated in Figure 5.



169 (a) Model 1  
 170 (b) Model 2  
 171 Figure 5: The two formulations resulting in Model 1 and Model 2. (a) For Model 1, the  
 172 entire saw body and cutting blade system is treated as rigidly connected. (b) For Model 2,  
 173 the cutting blade is treated as a separate rigid body connected by a pinned joint at O that is  
 174 assumed to have a negligible mass relative to the saw body. Note:  $I$  = moment of inertia  
 of the saw;  $M$  = mass of the saw body,  $m$  = mass of the cutting blade.

175 The first simplification, referred to as Model 1, treats the two bodies as  
 176 one combined rigid body. In this case, kickback force applied on the  
 177 cutting blade creates a linear force and a torque on the body, resulting in the  
 178 equations of motion seen in Equations (5) and (6).

179 
$$M\ddot{r}_c = F \tag{5}$$

180 
$$I\ddot{\theta} = -r_c \times F \tag{6}$$

181 The second simplification, referred to as Model 2, treats the cutting  
 182 blade as having negligible mass relative to the saw body. In this case, the  
 183 force applied to the blade during kickback through the pinch is transmitted

184 to the saw body through the center of rotation of the cutting blade, point  
185 O. Because the mass of the cutting blade is negligible, the full kickback  
186 force is seen by the saw body and is in the same direction that it would be  
187 on the cutting blade. In this case, the resulting equations of motions are  
188 slightly different, as seen in Equations (7) and (8).

$$189 \quad M\ddot{r}_c = F \quad (7)$$

$$190 \quad I\ddot{\theta} = r_{co} \times F \quad (8)$$

191 Unlike in Model 1, where the torque is based on the distance from the  
192 center of mass to the pinch point  $r_c$ , in Model 2 the torque is based only on  
193 the distance from the saw center of mass to the center of the cutting blade,  
194  $r_{co}$ . In both models, the same linear force is seen by the center of mass  
195 of the system, so the equation based on linear momentum (i.e. (5) and (7))  
196 does not change between them, and it is correct in general for the two body  
197 system.

198 The sets of Equations (5) and (6) and Equations (7) and (8) are  
199 independently numerically integrated with a MATLAB version R2018b  
200 solver to determine the evolution of the system and predict the theoretical  
201 bounds of the energy levels of the kickback event. The initial position and  
202 velocity of the saw body are sufficient initial conditions and are chosen to  
203 match the experiments.

204 The model has one tuning parameter, friction ( $\mu$ ), in addition to the  
205 measured parameters. This parameter is tuned since the cutting force is not  
206 well characterized for different materials at high surface speeds and pressures.  
207 Consequently,  $\mu$  is used to fit curves to data sets. It is found that as  $\mu$  is  
208 varied, Model 1 always predicts lower linear kinetic energy and higher  
209 rotational kinetic energy than Model 2, providing a pair of windows to fit  
210 experimental linear kinetic energy and rotational kinetic energy. The values  
211 used for  $\mu$  between each region of the saw, as illustrated in Figure 3, and the

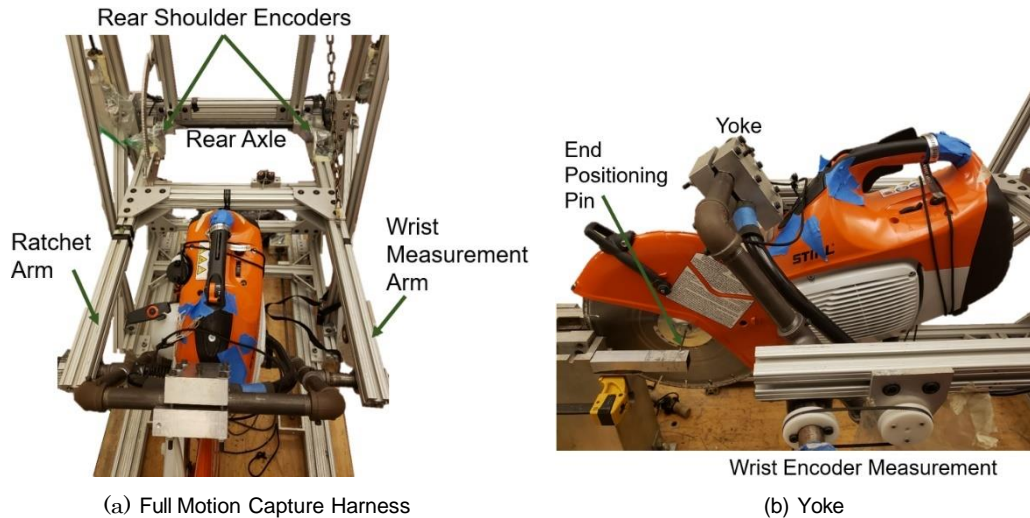
212 work material are 0.3 for Region I and 0 for Regions II and III. These values  
213 are used for modelling all of the saws tested under all test conditions.

## 214 *2.2. Test Machine*

215 A new type of kickback machine was designed built and tested to  
216 evaluate pinch based kickback. This machine has three major  
217 components: a floating center five bar linkage pneumatic piston actuated  
218 pincher which can apply a variable pinch force to the saw's cutting blade,  
219 producing kickback; a motion capture harness which allows for translation  
220 and rotation of the saw during kickback; and a positioning system which  
221 positions the saw relative to the pincher prior to initiating kickback.

### 222 *2.2.1. Motion Capture Harness*

223 The motion capture harness comprises of a pair of horizontal arms which  
224 hold the saw at their extremity, as seen in Figure 6. These arms can rotate  
225 about a fixed rear axle at their other extremity, allowing for translation of  
226 the saw's center of mass. The arms are sized such that this translation of  
227 the center of mass of the saw during engagement is approximately linear by  
228 a small angle approximation. Additionally, the arms are horizontal at the  
229 beginning of each kickback event such that the saw's initial translational  
230 motion is constrained to be entirely in the vertical direction. The saw itself  
231 is mounted in a yoke with a rotary axle oriented perpendicular to the cutting  
232 plane and aligned with the saw's center of mass, allowing for free rigid body  
233 rotation. Rotary encoders at both joints measure the rotational and  
234 translational position of the saw throughout kickback. The arms holding the  
235 saw yoke appear in Figure 6a, and a side view of the mounted saw yoke  
236 appears in Figure 6b.



237

(a) Full Motion Capture Harness

238

Figure 6: The motion capture harness used to hold the saw and measure the linear and rotational kinetic energy of the saw during the kickback event: (a) arms holding the saw yoke and (b) side view of the mounted saw yoke.

239

240

241

Although a majority of the energy in kickback is due to rotational motion, a linear degree of freedom allows for a more realistic trajectory of the saw during engagement, and kickback engagement changes when the saw's center of mass is allowed to move. Additionally, while the woodcutting saw kickback machine uses a horizontal degree of freedom [6], this linear degree of freedom was chosen to be vertical, as the kickback force was hypothesized to be primarily vertical for dangerous kickback. The woodcutting saw kickback machine uses a horizontal degree of freedom in order to reuse the mechanism which drives the coupon into the saw [10]; since the pinching mechanism used in this machine remains stationary, the direction of the linear degree of freedom can be changed.

242

243

244

245

246

247

248

249

250

251

252

### 2.2.2. Positioning System

253

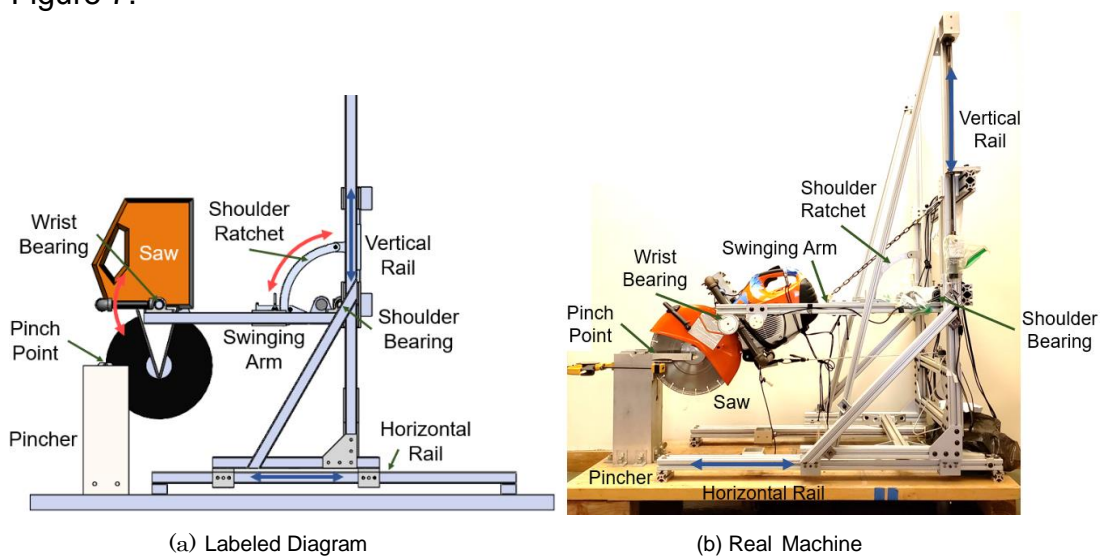
The motion capture harness is mounted on a mechanized Cartesian positioning system which moves the center of mass of the saw relative to the fixed pincher. The positioning system consists of two sets of linear rails, horizontal and vertical, with motion driven by parallel leadscrews, one

254

255

256

257 mounted on each rail. Encoder motors on each leadscrew position the saw  
 258 with a dual PID control loop. The leadscrews are selected to be non-back-  
 259 drivable, allowing them to hold position during kickback without requiring  
 260 active locking. Moving the motion capture harness and saw relative to the  
 261 pincher allows for the initial angle of the saw body  $\theta$  to be changed while still  
 262 engaging the pincher in a symmetric fashion and keeping the initial  $r_0$   
 263 horizontal. This setup aligns the initial kickback force with the vertical  
 264 degree of freedom. The positioning system also allows for saws of different  
 265 geometries to be tested while only requiring a change in the center of mass  
 266 coordinates based on the length from  $C$  to the  $O$  and the cutting blade  
 267 diameter. A labelled diagram and image of the full test machine appear in  
 268 Figure 7.

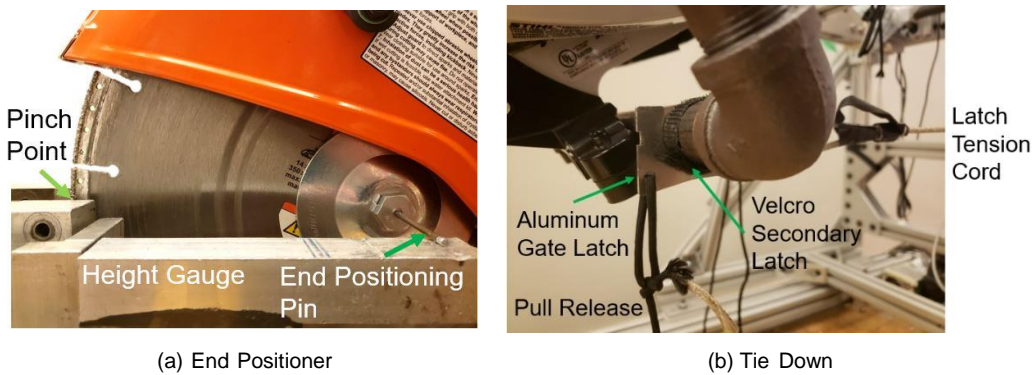


269 (a) Labeled Diagram (b) Real Machine  
 270 Figure 7: The test machine used in this study: (a) labeled diagram and (b) image of the  
 271 full test machine

272 An end positioner was mounted to the pincher to ensure that the center  
 273 of the cutting element is aligned horizontally with the pinch point at the start  
 274 of the engagement. This positioner also ensures that the initial angle of the  
 275 saw body is verifiable and that the cutting element is consistently positioned  
 276 relative to the work material. Given the small size of both the work material

277 and the abrasive region of the cutting blade, small variations in the initial  
278 contact angle could significantly affect the engagement of the cutting element  
279 during the pinch. This positioner and the locating pin on the saw appear in  
280 Figure 8a.

281 A two-part tie down is used to secure the saw in place while it is running  
282 prior to initiating kickback. The first part is a rigid latch which resists the  
283 initial kickback of the saw due to startup. It is released manually prior to  
284 initiating kickback. The second part is a breakaway connection which holds  
285 the saw in place until the initial kickback force releases it. The two-part  
286 tiedown appears in its fully engaged state in Figure 8b.



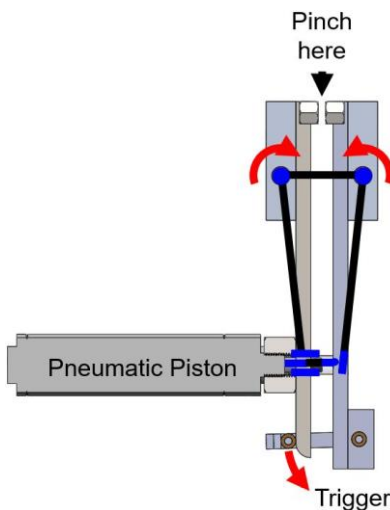
287 (a) End Positioner (b) Tie Down

288 Figure 8: (a) End positioner and (b) two-part tie down used to improve the repeatability  
289 of testing.

### 290 2.2.3. Pinching Mechanism

291 Theoretical predictions indicated that a pinching mechanism would need to  
292 be capable of applying up to 3 kN of normal force and be able to fully  
293 engage in less than 20 ms. Additionally, in order to evaluate the effects of  
294 different pinch forces on kickback, the pinch force would have to be able to  
295 be repeatedly varied. To meet these functional requirements, the pinching  
296 mechanism was designed as a pneumatic spring actuating a pair of levers  
297 to pinch the cutting blade. A long pneumatic cylinder is mounted to one  
298 lever and pushes on the other lever, while a hair trigger holds the two  
299 levers in place prior to kickback. The levers are mounted with widely spaced

300 bushings to provide the force couple needed to resist moments, allowing  
301 for proper resistance of both vertical and horizontal kickback reaction  
302 forces. Single use pinch pads, made from hexagonal stock to resist twisting  
303 in their seats, are used to emulate the kerf work material and are mounted  
304 to the tops of the levers to directly pinch the saw blade. A diagram  
305 illustrating the inner workings of the pinching mechanism appears in Figure  
306 9. The pinching mechanism is housed in a 6 in. by 6 in. by ½ in. 6061  
307 aluminum square tube which provides structural rigidity for the system. A  
308 slit in the front and back of the top of the housing allows for the saw blade  
309 to swing through the housing.



310 Figure 9: Labelled diagram showing internal components of the pinching mechanism.

311 A pneumatic system is used for adjustable high-force generation.  
312 Varying the pressure in the piston linearly varies the pinch force.  
313 Additionally, pre-pressurizing the piston and holding the mechanism open  
314 with a hair trigger allows for fast actuation without being limited by air flow  
315 rates as the piston undergoes adiabatic expansion. A 2 in. diameter, 5 in.  
316 long piston cylinder was chosen. The diameter of the piston was chosen to  
317 achieve appropriate pinch forces, and the length was chosen to be much  
318 longer than the required stroke. The piston rod was cut short so that the  
319 piston always operates more than 90% extended, thereby limiting the

320 maximum pressure loss due to adiabatic expansion. Moreover, for all  
321 cutting elements of the same thickness, the pressure loss is the same.

322 Levers were sized to provide an additional 3x force multiplication of the  
323 piston. These levers are configured in a class 1 lever configuration, allowing  
324 for the pinch point to be at the top of the pinching mechanism, while the  
325 rest of the hardware resides safely below the path of the saw blade. The  
326 lower part of the levers forms a 5-bar linkage, with the end of the pneumatic  
327 piston able to slide on the surface of one lever, allowing for centered force  
328 application. Unlike in a common 5-bar linkage, like a set of bolt cutters, two  
329 links are replaced by the pneumatic piston and its extending rod. This design  
330 allows the saw blade to be symmetrically pinched in a repeatable fashion.

331 At the output of the pinching mechanism, single use pinch pads are  
332 mounted to directly engage the saw blade. These pinch pads are turned  
333 on a screw machine from  $\frac{3}{4}$  in. hex stock with a 1/4-20 tapped hole through  
334 their central axis. They are mounted to the levers using 1/4-20 bolts.  
335 Additionally, shelves were milled out of the levers to provide vertical force  
336 transmission and to hold the pinch pads irrotationally.

### 337 *2.3. Testing Protocol*

338 To prepare a saw for testing, the saw is mounted in a harness that  
339 allows it to rotate freely about its center of mass. For each test, the  
340 machine repositions the saw's center of mass such that the cutting element  
341 is centered in the pinch point and the initial contact angle of the saw is as  
342 desired. The saw is then locked in position with the two-part tie down. Next,  
343 the saw is started and allowed to reach full speed. Then the pinch is  
344 engaged, generating the kickback. The rotational and translational  
345 positions of the saw are recorded by the motion capture harness during  
346 kickback. A hard stop prevents the saw from rotating beyond a directly  
347 vertical orientation, and upon reaching this position the saw throttle is



348 released. The saw is then prepared for the next trial. The testing conditions  
349 and protocols are adapted to the specific saws as follows:

### 350 *2.3.1. Electrical Circular Cutoff Saw*

351 The kickback machine was initially tested in a shielded indoor  
352 laboratory environment with an electric circular cutoff saw (ECCS). With  
353 the ECCS, initial testing was conducted at a single pressure and a single  
354 contact angle to verify the consistency and accuracy of the data collected.  
355 Afterward, extensive testing of the ECCS was used to test the sensitivity  
356 of the physics model. Data was primarily grouped into sweeps across a  
357 range of initial contact angles. The initial contact angle was swept through  
358 for tests using different diameter blades and with multiple different pinch  
359 forces. The resultant data was compared to the predictions from the  
360 model.<sup>1</sup>

### 361 *2.3.2. Gas-Powered Saws*

362 The gas-powered saws were tested in an outdoor environment. The  
363 circular cutoff saw was used without water cooling, while the chainsaw was  
364 used with water cooling. Each saw was initially filled with the appropriate  
365 50:1 gas-oil fuel mixture and refilled after each set of three trials. Also, the  
366 chain was re-tensioned each time the chainsaw was refueled. The results  
367 of the gas-powered saw testing are used to show kickback energy of  
368 industrial saws, as well as to compare the resultant kickback energies of  
369 the two saws. Results and Discussion

### 370 *3.1. Kickback Machine Validation*

371 The ECCS was used for the initial validation of the test machine since  
372 it allowed for a simpler and more consistent test setup and procedure. This  
373 saw did not require water cooling or special ventilation, allowing it to be

---

<sup>1</sup>Testing was also performed with a cutterless electric woodcutting chainsaw; however, the lack of an abrasive cutting region made the results chaotic and unreliable.

374 tested indoors. Also, the saw body was rigidly attached to the harness,  
375 simplifying the system. Further, the electric motor produced less vibration  
376 and pulsation, could be powered on and off by a switch, and did not cause  
377 any change in mass during testing (unlike the consumption of gas during the  
378 gas-powered saw operation).

### 379 *3.1.1. Overall Machine Repeatability*

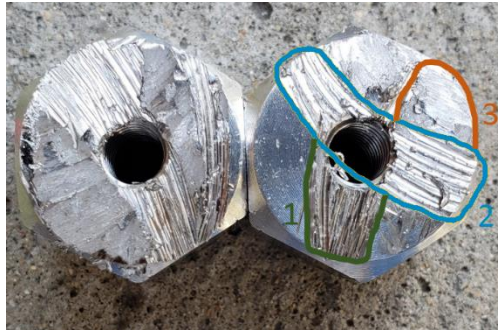
380 The kickback machine was tested for repeatability to determine the overall  
381 error attributable to the test machine itself. Testing consisted of verifying the  
382 linear encoder measurements and producing nine kickbacks with the ECCS  
383 using a 12 in. diameter blade. The blade was pinched with a pinch force of  
384 1260 N and an initial contact angle of 20°. The linear, rotational, and total  
385 mechanical energies were found to have relative standard deviations of 6.9%,  
386 11.4%, and 7.5% respectively. These results, which can be seen in  
387 Appendix A.1, increase confidence that variation seen in the data is not  
388 primarily due to factors from the test machine. Further, the measured  
389 resultant kickback energy values were of the same order of magnitude of  
390 the kickback energy found in woodcutting saw tests done by Dąbrowski  
391 [10], demonstrating that the kickback event generated is representative of  
392 dangerous kickback that can occur during normal saw operation.

### 393 *3.1.2. Work Material*

394 For testing in this investigation, 6061 aluminum and mild steel pinch pads  
395 were used. However, in the future, additional materials could be used. An

396

example of used 6061 aluminum pinch pads appears in Figure 10.



397

Figure 10: Pinch pads used during testing. Note: 1, the initial cut by the abrasive edge; 2, a second area of engagement during the kickback event; 3, the area contacting Region II of the saw.

398

399

400

A majority of testing was performed with 6061 aluminum pinch pads due to its ease of manufacture and theorized high  $\mu$  when engaged with diamond abrasive cutting surfaces. The cutting application being examined, however, was the cutting of ductile iron pipe. Thus, mild steel pinch pads were fabricated and used to compare to the tests with aluminum pinch pads. This testing did not show a significant difference in the data produced using each material, as seen in Figure 11.

401

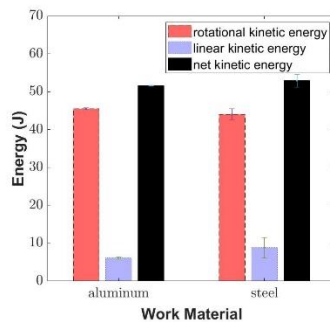
402

403

404

405

406



407

Figure 11: Comparison in measured kickback energy using steel and aluminum work material. Note: The error bars indicate the range of measured values.

408

409

While aluminum pinch pads were primarily used material for testing, some gas-powered saw trials conducted using mild steel pinch pads resulted in the observation of notable trajectories. These tests showed an initial kickback energy at or slightly below the observed levels from the aluminum

410

411

412

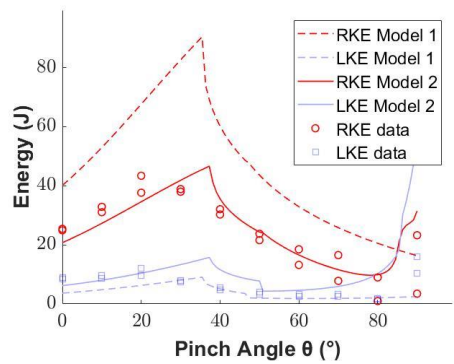
413 pad tests. However, the blade had more difficulty disengaging from the  
414 pinch point. This effect is amplified by the compliance of the vibration  
415 isolator springs in the gas-powered saw harnesses, allowing the saw to  
416 move such that the abrasive remains engaged in the pinch point while the  
417 motion capture harness moves separately. This total motion is not fully  
418 observed by the motion capture harness, as the linear component of the  
419 force vector starts to align with the horizontal, so its contribution is not fully  
420 measured. Because the initial kickback energy before this extra motion  
421 matches the energy levels observed during testing with aluminum as a work  
422 material, the testing with aluminum pinch pads remains valid for evaluating  
423 the kickback energy of these saws during ductile iron pipe cutting.

### 424 3.2. *Model Validation*

425 The ECCS was also used to validate the model conclusions for the  
426 reasons outlined above in Section 3.1. The independent parameters tested  
427 for model validation included initial contact angle, cutting blade diameter,  
428 and pinch force.

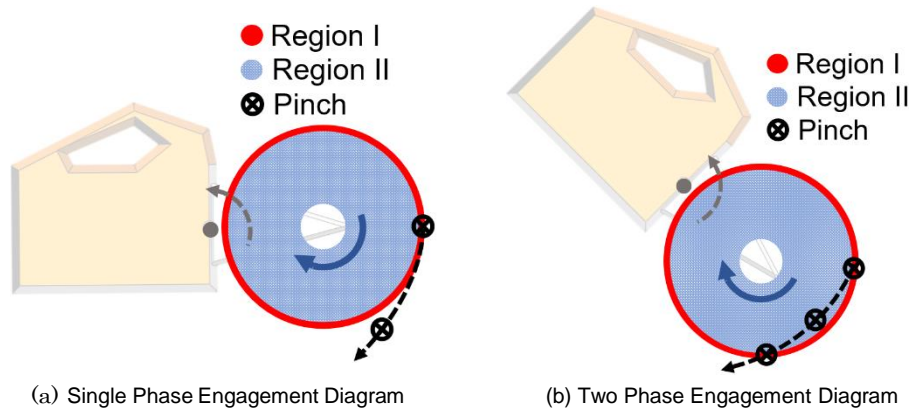
#### 429 3.2.1. *Initial Contact Angle Sensitivity*

430 The first model parameter examined was the initial angle of the kickback,  
431  $\theta$ , shown in Figure 4. In the field, initial contact angle varies widely with  
432 how the user is holding the saw and the cut they are making, indicating the  
433 importance of characterizing its effect on kickback. For almost all tested  
434 combinations of saws, blade diameters, and pinch forces, the kickback energy  
435 tends to increase as the initial angle increases, reach an abrupt peak at a  
436 specific angle, and then rapidly decreases again. This phenomenon  
437 agrees with predictions by the model and can be seen in Figure 12.



438 Figure 12: Sample dataset compared with the model prediction for the ECCS with a 12 in.  
 439 diameter blade and a pinch force of 1680N. Note: ECCS = electric circular cutoff saw;  
 440 RKE = rotational kinetic energy; LKE = linear kinetic energy.

441 Examinations of the simulation and of used pinch pads indicate that a  
 442 transition in the nature of the engagement between the cutting blade and the  
 443 work material occurs around the angle corresponding to the peak kickback  
 444 energy. The contact transitions from a *single-phase engagement* to a  
 445 *dual-phase engagement*. Single-phase engagement refers to when the  
 446 work material maintains continuous engagement with the abrasive region  
 447 of the cutting blade throughout the engagement part of the kickback event,  
 448 as illustrated in Figure 13a. Dual phase engagement refers to when the  
 449 work material engages the abrasive region of the cutting blade during two  
 450 discrete times in a single kickback, as illustrated in Figure 13b. The first  
 451 engagement with the abrasive region of the saw occurs at initiation and ends  
 452 when the saw moves so that the work material engages the low-friction  
 453 interior of the cutting blade/saw bar (Regions II and III). The second  
 454 engagement occurs when the saw moves such that the work material  
 455 reengages the abrasive region of the saw, and it ends when the saw fully  
 456 separates from the work material.



(a) Single Phase Engagement Diagram

(b) Two Phase Engagement Diagram

457  
458  
459

Figure 13: The path the pinch point traces on the blade relative to the motion of the saw during (a) single-phase and (b) dual-phase engagement.

460  
461  
462  
463  
464  
465  
466  
467  
468

This change in abrasive engagement provides a physical explanation for the change in the resultant kinetic energy of the saw. The linear friction approximation implies that the engagement region with the highest coefficient of friction, the abrasive, could dominate the kickback event. As the initial angle increases from zero, the work material remains engaged with the abrasive region over a longer distance. However, when the transition from single to dual engagement occurs, the length of the work material engagement with the abrasive region becomes shorter, and it further decreases as the initial angle continues to increase.

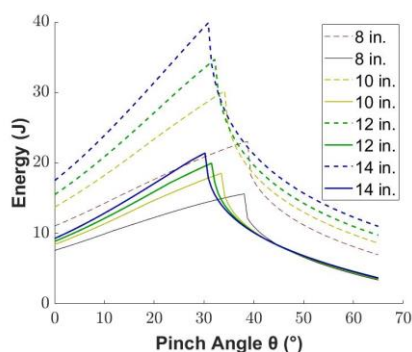
469  
470  
471  
472  
473  
474

The observation of this trend in kickback energy in both the experimental data and the model predictions supports the validity of the model. Moreover, the observation of the suspected cause, a shift from single to dual phase engagement, in both experimental data and the model predictions further indicates that the model is capturing a characteristic behavior of pinch-based kickback.

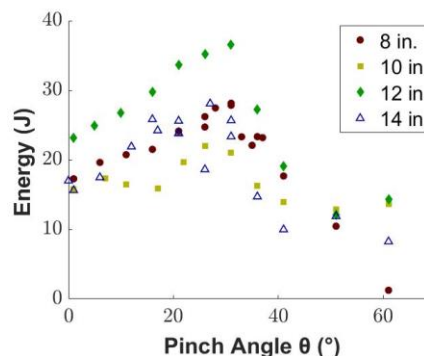
475

3.2.2. *Blade Diameter Sensitivity*

476 The cutting blade diameter was selected as a test variable as it represents  
 477 one of the most easily and often changed parameters of a saw.  
 478 Additionally, as the cutting blade diameter increases, both the area which  
 479 presents a kickback risk and the length of a potential engagement  
 480 increase, leading to an expected increase in the kickback risk [11]. The  
 481 cutting blade diameter is also one of the main differences between how  
 482 the model treats a chainsaw and a circular cutoff saw. To test the model's  
 483 prediction for the effect of changing the saw blade diameter on the resultant  
 484 kickback energy, the ECCS was tested with four different diameter blades.  
 485 According to the model, the kickback energy should increase as the  
 486 diameter of the blade increases. Also, for larger diameters, the peak energy  
 487 should occur at a smaller initial contact angle. These predicted trends are  
 488 related to the change in the length of the abrasive region engaged by the  
 489 work material as the diameter of the blade changes. These predictions are  
 490 shown in Figure 14a. The broken lines represent the predictions of Model 1,  
 491 while the solid lines represent the predictions of Model 2.



492 (a) Model predicted effect of different diameter  
 493 testing.



494 (b) Measured data from different diameter blade  
 495 testing.

496 Figure 14: Comparison of the predicted (a) and measured (b) change in kickback energy for an  
 497 increase in the diameter of the blade. Note: Broken lines, prediction by Model 1; solid lines  
 498 prediction by Model 2. Data for the 8 in. and 12 in. blades are close to the Model 2  
 499 predictions, while data for the 10 in. and 14 in. blades are closer to the Model 1  
 500 predictions.

499           The collected data does not show either of these expected changes,  
500           contradicting the expected result [11] of an increase in kickback energy  
501           with blade diameter; instead, all four sets of data show that the peak energy  
502           occurs around the same contact angle, near 30°, and the smallest and  
503           largest diameter blades produce similar, medium levels of kickback energy.  
504           Additionally, while the kickback energy observed during testing with the 8  
505           in. and 12 in. diameter blades agree more with the predictions of Model 1,  
506           the results from testing the 10 in. and 14 in. diameter blades are closer to  
507           the predictions of Model 2. This observation suggests that the accurate  
508           model of the saw would be somewhere between the simplifications made  
509           in each model.

510           One potential explanation for this observed discrepancy is that the blades  
511           differed in abrasive patterning, shown in Figure 15.



512           Figure 15: Different abrasive patterns on the different diameter blades.

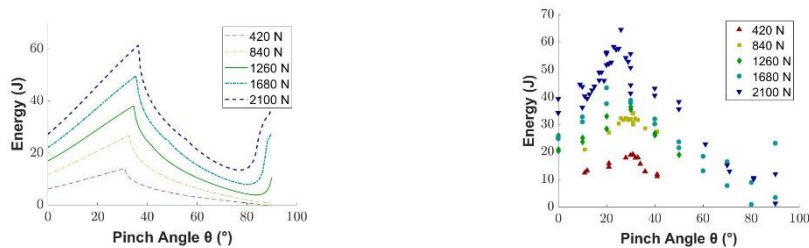
513           Notably, the 8 in. and 14 in. diameter blades have a similar abrasive  
514           pattern and produce similar levels of kickback, indicating that the abrasive  
515           pattern could be more significant than the blade diameter in determining  
516           kickback energy. However, further testing using blades with different  
517           diameters and the same abrasive pattern, as well as blades of the same  
518           diameter with different abrasive patterns, would be necessary to verify this  
519           claim. This further testing would also be necessary to validate the  
520           observation that the two models seem to bound the resultant energy, as  
521           the abrasive pattern could have an overriding, unobserved effect.



522 3.2.3. Pinch Force Sensitivity

523 To further test the model's predictions, the pinch force used to generate  
524 the kickback was varied while keeping the blade diameter constant. The  
525 pinch force represents an environmental condition, so changes in kickback  
526 energy during this testing represent how the model predicts changes in  
527 response to the conditions creating the kickback. Since the actual pinch  
528 force in practice can vary, this quantity would not be known in advance for  
529 kickback energy prediction in the field. However, this analysis can be used  
530 to demonstrate the potential danger of the kickback under progressively  
531 more dangerous conditions.

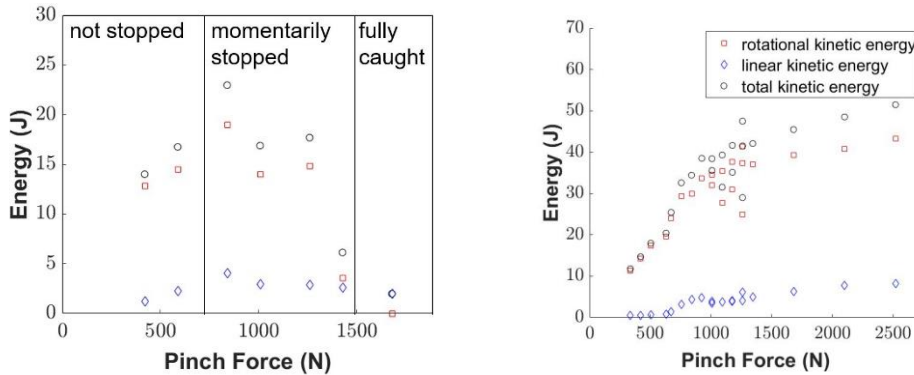
532 Because the modeled kickback force is much larger than gravity, the  
533 model predicts that the kickback energy should increase linearly with pinch  
534 force. Changing the magnitude of the pinch force changes the rate at which  
535 the saw translates and rotates, but the spatial trajectory of the saw remains  
536 the same. The corresponding data, seen along with this prediction in Figure  
537 16, shows the expected increase in kickback energy as normal force  
538 increases. However, the observed increase is not definitively linear. The  
539 increase is rapid from a low to medium force, then slow for the next two  
540 incremental increases, then rapid again to the highest applied force.



541 (a) Model predicted effect of different pinch force testing  
542 (b) Measured data from different pinch force testing.

543 Figure 16: Comparison of the predicted (a) and measured (b) change in kickback energy for  
544 an increase in the normal force on the blade. Note: (a) Only Model 2 predictions  
545 presented to illustrate the trend as pinch force increases. Model 1 predictions follow a  
546 similar trend but at lower magnitudes.

547 Further testing of increasing the normal force was performed with two other  
 548 blade diameters: the 8 in. and 14 in. diameter blades. Again, the model predicts  
 549 that the kickback energy should increase linearly as normal force increases. The  
 550 data for these experiments appears in Figure 17.



551 (a) 8 in. Diameter Blade, 0° Initial Angle                      (b) 14 in. Diameter Blade, 30° Initial Angle

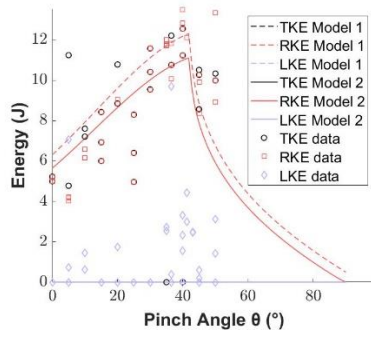
552 Figure 17: Increasing pinch force with a constant diameter blade and initial contact angle. Note:  
 553 (a) shows that increasing the pinch force, the initial resultant kickback energy is linear,  
 554 as predicted by the model. However, once the pinch force is high enough to cause the  
 555 blade’s motion to come to a momentary stop, the kickback energy begins to decrease,  
 556 until the saw is completely caught in the pinch and there is no kickback. (b) Testing with  
 557 a larger diameter blade shows a similar initial linear increase in resultant kickback energy,  
 558 but it does not show a later decrease in resultant kickback energy. Instead, there is a  
 559 transition to a less steep linear slope. Region labels in (a) refer to whether the cutting  
 560 blade was caught in the pinch point during the kickback event (either not at all, momentarily  
 561 caught then released, or fully caught and stopped). Labels in (b) also apply to (a).

562 For both blades, the increase is initially linear. However, testing with  
 563 both diameter blades indicate the existence of a transition point, after which  
 564 the behavior changes. For the 8 in. blade, this behavior is associated with  
 565 stopping of the blade during the kickback, though the saw body would keep  
 566 moving, as revealed by high-speed video. This continued motion would  
 567 enable the saw to pull itself loose and start spinning the blade again, so the  
 568 kickback event would continue. However, this instantaneous stop would  
 569 reduce the resultant energy with which the saw would leave the  
 570 engagement point. This data represents a limitation of the model, as the

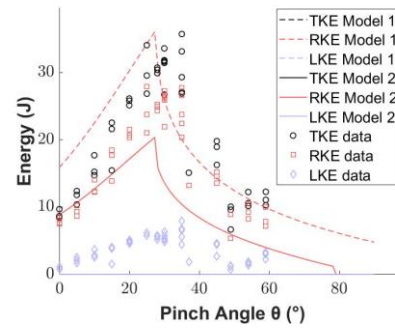
571 model does not allow for changes in the speed of the blade. The maximum  
572 energy appears to correspond to the point at which the blade is first  
573 stopped. This point indicates when no additional energy can be extracted  
574 from the blade. For the 14 in. blade, the kickback energy continues to  
575 increase linearly, albeit at a much lower rate. High speed video was not taken  
576 during this testing, so it cannot be verified whether there is also an  
577 instantaneous stopping of the blade at/after this transition point.

### 578 3.3. *Gas-Powered Saw Testing*

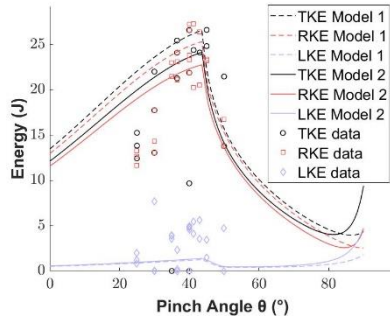
579 After testing the strengths and limitations of the model's predictions,  
580 the test machine was used to measure the kickback energy for two  
581 industrial gas-powered saws, the circular cutoff saw and the abrasive  
582 chainsaw. Both of these saws exhibit the same kind of peaked curve of  
583 kickback energy with respect to contact angle as found with the ECCS,  
584 agreeing with the model. This data and the corresponding model  
585 predictions are shown in Figure 18. It is observed that when pinched with  
586 higher forces, the chainsaw has significantly more variability in the measured  
587 kickback energy than the cutoff saw. This variability is likely due to the  
588 nonuniformity of the diamond abrasive chain, which has abrasive on  
589 opposite sides of every other chain link. Since the collected data is  
590 reasonably close to the predictions from the model, it is valid for comparing  
591 the kickback safety risk of these two types of saws. Plots comparing the  
592 measured kickback energy of these two saws at three different pinch force  
593 levels appear in Figure 19.



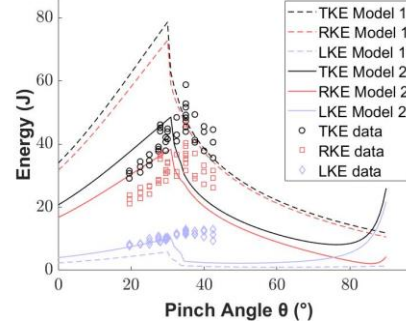
(a) Chainsaw 588N Data vs Model



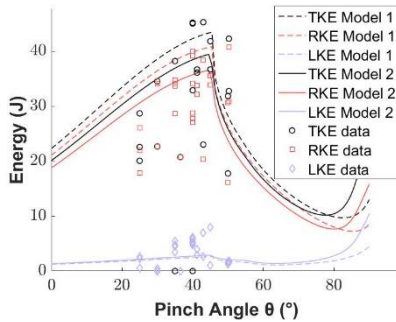
(b) Circular Cutoff Saw 588N Data vs Model



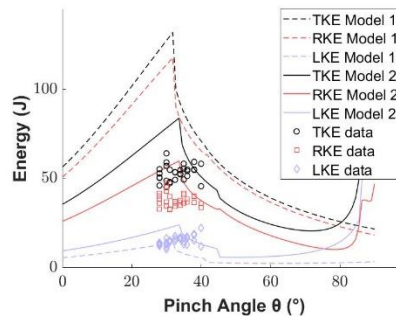
(c) Chainsaw 1260N Data vs Model



(d) Circular Cutoff Saw 1260N Data vs Model



(e) Chainsaw Saw 2100N Data vs Model



(f) Circular Cutoff Saw 2100N Data vs Model

594

595

596

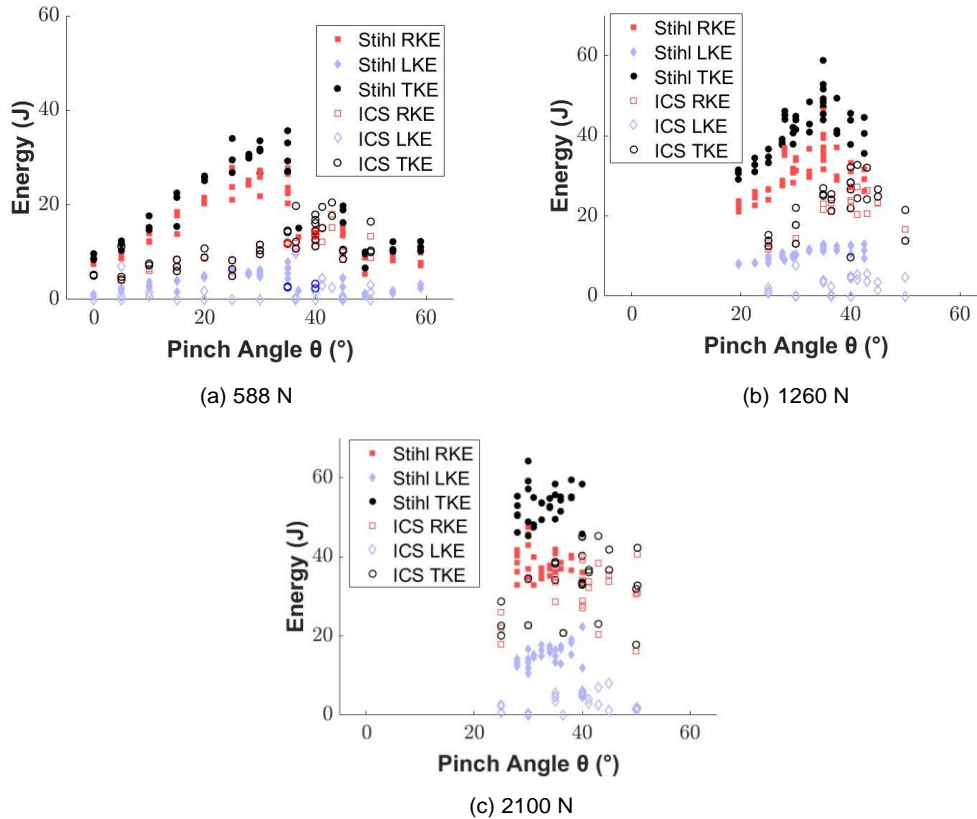
597

598

599

600

Figure 18: Subfigures a-f compare the measured kickback energy data to the model predicted kickback energy for the chainsaw(a,c,e) and the circular cutoff saw (b,d,f) at three different pinch force levels: 588 N (a,b), 1260 N (c,d), and 2100 N(e,f). Note: LKE = linear kinetic energy; RKE = rotational kinetic energy; TKE = Total kinetic energy.



601

602

603

604

605

Figure 19: Comparison of the kickback energy data for the circular cutoff saw (Stihl TS420; Stihl USA, USA) and the chainsaw (ICS 695XL; Blount International, USA) for angle sweeps at three different normal force levels: (a) 588 N, (b) 1260 N, and (c) 2100 N.

606

607

608

609

610

611

612

613

614

615

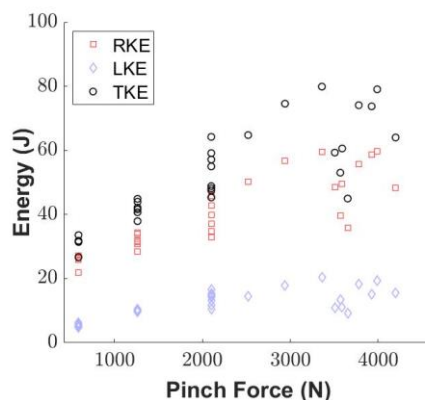
616

These plots show that the two saws generate peak kickback energy at two different initial contact angles, as anticipated by the model. At the chainsaw's peak energy, around an initial contact angle of 42°, the rotational kinetic energy is comparable to that of the circular saw, given the same initial contact angle. However, because the circular saw has a greater linear kinetic energy at nearly all initial contact angles, particularly as the normal force increases, the total kickback energy (for equal weighting of linear and rotational kinetic energy) is greater for the circular saw. For initial contact angles larger than 42°, the rotational kinetic energy of both saws is expected to remain similar, as the energy level of both saws would decrease. At lower initial contact angles, all energy

617 measurements are higher for the circular saw, including at the circular  
618 saw's peak energy around an initial contact angle of 30°.

### 619 3.3.1. High Pressure Testing

620 While testing with a pinch force of 2100 N started to occasionally catch  
621 the nose of the chainsaw such that it remained stuck in the pincher rather  
622 than kicking back, these tests did not result in the circular cutoff saw blade  
623 being caught. Since testing with the ECCS verified that further increasing  
624 pinch force would increase the resultant kickback energy, the circular cutoff  
625 saw was also tested at higher pinch forces to approach an experimental  
626 maximum kickback energy. The results of this testing, appearing in Figure  
627 20, indicate that the resultant energy increases to a plateau, then begins to  
628 decrease as pinch force continues to increase. While high-speed video  
629 does not capture any momentary catching of the saw blade during these  
630 tests, this data indicates that there is a finite limit to how much energy can  
631 be transferred to saw motion during kickback.



632 Figure 20: High Pressure testing for the circular cutoff saw with an initial contact angle of  
633 31°.

### 634 3.3.2. Vibration Isolator Effects

635 Both of the gas-powered saws have vibration isolator springs between  
636 the saw body and the saw handle. Analysis of high-speed video indicated

637 that the compliance of these springs allowed for a difference in the rigid  
638 body motion of the saw itself and the motion of the handle, which is  
639 measured by the harness. Since the springs are conservative, any energy  
640 stored in the springs would create oscillations in the motion of the handle and  
641 the rigid body. The frequency of these oscillations observed in the data  
642 could be measured and compared to the natural frequency of the saw-  
643 spring-handle system. The measured and predicted frequencies matched  
644 to within 10% error.

645 The measured amplitude of these oscillations indicates the displacement  
646 of the springs, from which the stored energy can be calculated. Based on  
647 the measured stiffness of the springs, the calculated stored energy was  
648 about 0.05 J for each saw. This level of energy storage confirms that the  
649 kickback energy is primarily transmitted into rigid body motion, rather than  
650 into the vibration isolators. Hence, the effects of the vibration isolators can  
651 be neglected.

### 652 3.3.3. *Stopping the Cutting Element*

653 As mentioned in Section 2.1.2, the model assumes a constant speed  
654 for the cutting blade. While this assumption would allow kickback energy  
655 to increase with pinch force without an upper limit, this case does not  
656 match observations. Experimental results demonstrate that this assumption  
657 starts to break down as the pinch force increases and the cutting blade  
658 diameter decreases. The 8 in. diameter blade was observed to have stopped  
659 instantaneously during some kickback trials, but a lack of high-speed video  
660 analysis for other diameter blades or the gas-powered saws prevents  
661 confirmation as to whether the same phenomenon occurs for those blades  
662 or the chainsaw chain given the tested conditions. However, the entire saw  
663 tip was stopped and caught during some of the chainsaw testing, indicating  
664 that the chainsaw was nearing a potential maximum possible energy, as a

665 blade caught in the work material would not kick back. In this case, the  
666 pinching work material absorbs all of the kickback energy, stopping both  
667 the motion of the cutting element and the saw body. This phenomenon  
668 differs from the use of a chain or blade brake to prevent kickback, as the  
669 kickback energy is typically completely transferred to the saw/operator  
670 before the brake is actuated. Further testing at higher pinch forces, along  
671 with high speed video analysis, would allow for identifying the upper  
672 boundary of kickback energy of a saw for unknown pinch conditions.

### 673 **3. Conclusions and Future Work**

674 This work demonstrates that pinch-based abrasive saw kickback can have  
675 energy levels comparable to woodcutting saw kickback, even though the  
676 kickback mechanism differs. The friction-based model used for analyzing  
677 kickback of abrasive saws captures the abrasive saw kickback  
678 phenomenon and can be used to provide an initial expectation for the  
679 kickback energy potential of a given saw. Additionally, the designed and  
680 developed test machine can repeatedly and accurately measure the  
681 kickback energy produced by a given saw. Furthermore, the results  
682 indicate that the parameters of a chainsaw generate less energy than those  
683 of a circular saw given the same kickback conditions. The increased risk due  
684 to the high measured and predicted kickback energy of the circular cutoff  
685 saw is amplified by the fact that cutting pipe in an excavated trench with a  
686 circular cutoff saw requires the kickback zone to be engaged to completely  
687 cut through a pipe. The model and test machine developed in this work  
688 indicate that pinch based kickback can present a safety risk for operators  
689 of abrasive saws, and this work provides a reliable method for measuring  
690 this risk. It is envisioned that the model together with the test apparatus can  
691 help manufacturers develop safer saws in a deterministic manner.

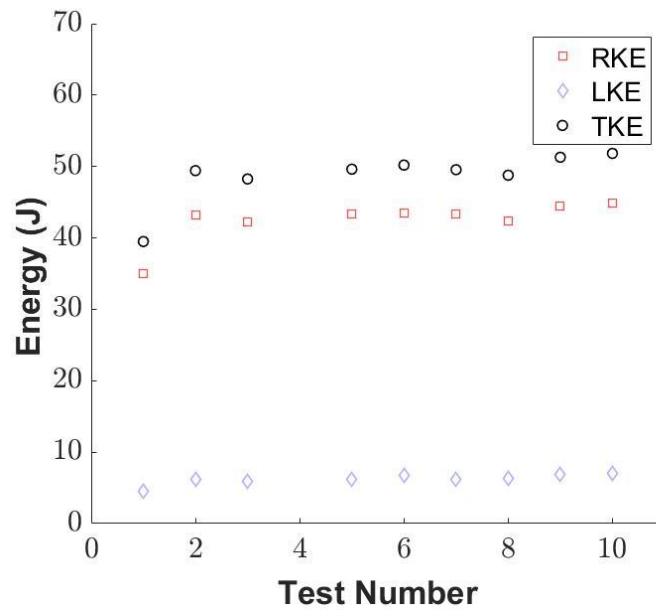


692 Future work should include more data collection for saws with different  
693 abrasive patterns and the same diameter blade, as well as the same  
694 abrasive patterns on different diameter blades to investigate the effect of  
695 abrasive patterning on resultant kickback energy. Additionally, more data  
696 can complete the angle sweeps performed with the gas-powered saws to  
697 develop a more complete picture of the kickback behavior, particularly at  
698 higher pinch forces. Also, the effect of different work materials could be  
699 investigated further using materials with extreme properties (such as  
700 Teflon, which has a high shear strength but a low coefficient of friction).

701 **Appendix A. Machine Repeatability**

702 *Appendix A.1. Data from Repeatability Testing*

703 The test data used to determine the overall repeatability of the test  
704 machine appears in Figure A.21. While this data indicates that the overall  
705 machine produces consistent data, the linear kinetic energy measurements  
706 were shown to be much lower than the rotational kinetic energy  
707 measurements. Because of the relatively low magnitude of these linear  
708 kinetic energy measurements, it was deemed important to verify the  
709 accuracy of these measurements with a secondary measurement system.  
710 This verification is discussed in Section Appendix A.2.



711 Figure A.1: Plot of the rotational, linear, and total kinetic energy for multiple tests of the  
712 same test setup. Test 4 encountered a recording error and has been omitted.

713

### Appendix A.2. Linear Kinetic Energy Measurement

714

Given the arms' relatively small angular displacement during saw

715

translation, the position data measured generally has low resolution. The

716

system's accuracy was measured by mounting a laser on top of one arm

717

on the end opposite the pivot point of the arm. The laser was oriented to

718

shine along the arm's length and project onto a surface a half meter away.

719

A camera was used to track the motion of the projected dot throughout nine

720

kickback trials, and the angle of the arms at each point was calculated

721

based on the measured data. The measurement of the arm's position with

722

the laser appears with the encoder measurements in Figure A.22a. The

723

peak linear velocity was calculated using the encoder measurement and

724

compared to the velocity calculated using the laser measurement. This

725

comparison is shown in Figure A.22b. On average, the encoder measured

726

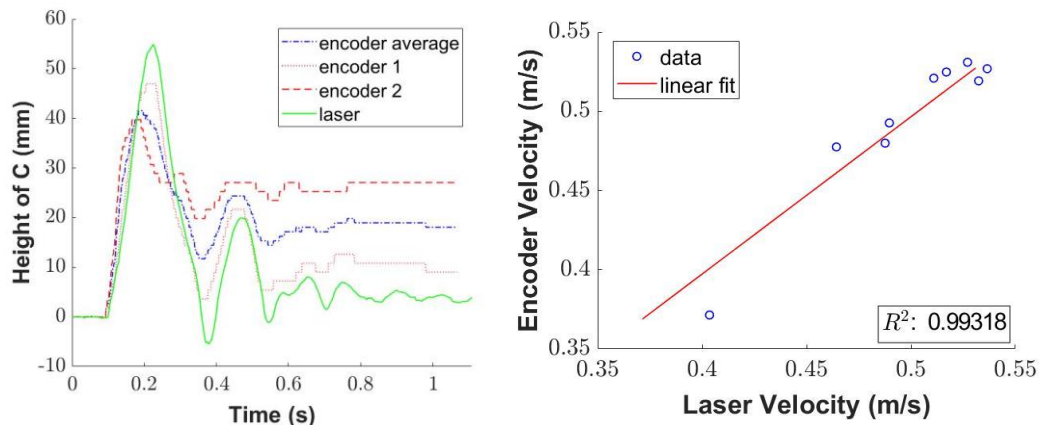
velocity was within 99.3% of the laser measured velocity, supporting the

727

conclusion that its resolution and accuracy were high enough to measure

728

the linear velocity of the saw.



729

(a) Data from the encoders on each arm compared with the laser measurement. (b) Correlation between the data measured from the laser and the encoder.

730

731

Figure A.2: Comparison of laser-measured and encoder-measured linear position data: (a)

732

representative of one trial and (b) summarized correlation over nine trials. Note: C =

733

center of mass of the saw. The laser was mounted to the arm whose position is measured

734

by Encoder 1.

## References

- [1] Koehler SA, Luckasevic TM, Rozin L. Death by chainsaw: fatal kickback injuries to the neck. *J Forensic Sci.* 2004;49(2):345–50.
- [2] Haynes CD, Webb WA, Fenno CR. Chain saw injuries: review of 330 cases. *J Trauma.* 1980;20(9):772–6.
- [3] Arnold D, Parmigiani J. A Method for Detecting the Occurrence of Chainsaw Kickback. *Dyn. Syst. and Control; Mechatron. and Intell. Machines, Parts A and B, ASMEDC.* 2011;7:441–447.
- [4] Robinson D. Evaluation of chain saw simulated kickback modes. *Cent. Manuf. Eng. (MD): National Bureau of Standards (US); 1984.* (NBSIR publication; no. 84-2823).
- [5] Commission Approves Mandatory Approach Toward Reducing Chain Saw Injuries From “Kickback”. *Consumer Products Safety Commission (US); 1980.* (CPSC release; no. 80-023).
- [6] American National Standards Institute (ANSI)/Outdoor Power Equipment Institute (OPEI). *Internal Combustion Engine-Powered Hand-Held Chain Saws – Safety and Environmental Requirements.* New York: ANSI/OPEI; 2014. Standard No. B175.1-2012
- [7] Wu J. Theoretical investigation of kickback in diamond chainsaw and circular cut-off saw [master’s thesis]. Cambridge (MA): MIT; 2018.
- [8] Yue BJ. Evaluation of kickback energies in abrasive chain saws and cut-off saws: a theoretical and experimental study [master’s thesis]. Cambridge (MA): MIT; 2019.
- [9] Arnold D, Parmigiani JP, A Study of Chainsaw Kickback. *For. Prod. J.* 2015;65(5-6):232–238.

- [10] Dąbrowski A. Kickback risk of portable chainsaws while cutting wood of different properties: laboratory tests and deductions. J Occup. Saf. Ergon. 2015;21(4):512–23.
- [11] Chainsaw Kickback Explained: Learn How to Avoid The Danger [Internet]. c2019. Available from: <https://www.oregonproducts.com/en/chain-saw-kickback>.